Memory and persistence correlation of microstructural fluctuations in two-dimensional dusty plasma liquids

Yu-Hsuan Huang and Lin I
Department of Physics and Center for Complex Systems, National Central University, Jhongli, Taiwan 32001, Republic of China
(Received 31 January 2007; revised manuscript received 9 May 2007; published 10 July 2007)

We investigate the temporal memory and persistence time correlations of microstructural order fluctuations in quasi-two-dimensional dusty plasma liquids through directly monitoring particle positions. The persistence length of the ordered and the disordered microstates both follow power-law distribution for the cold liquid. The correlation probabilities of the persistence lengths in different pairs of fluctuating cycles show that an order-disorder-order and a disorder-order-disorder sequence are more likely to have the long-short-long or short-long-short persistent lengths combination. The persistence time correlation lasts for several fluctuating cycles. The correlation memory is stored in the surrounding heterogeneous network through mutual coupling. Increasing thermal noise level deteriorates the memory and leads to the less correlated stretched exponential distribution of the persistent length.

DOI: 10.1103/PhysRevE.76.016403 PACS number(s): 52.27.Lw, 05.70.Ln, 05.40.−a, 61.20.−p

I. INTRODUCTION

At the discrete microscopic level, liquid can be treated as a coupled many-body system driven by stochastic thermal noise [1–5]. Very little is known about its rich fluctuating dynamics which is not completely random under strong mutual coupling. Recently, the development of the dusty plasma liquid, a Coulomb liquid formed by the charged micrometer particles suspended in low pressure discharges, provides an inspiring experimental platform with proper scale for addressing this issue through direct optical visualization of the spatiotemporal evolutions of particle positions [5–10]. In this work, using the idea of persistence and introducing a measurement for the correlation of the successive persistence times, we experimentally explore the temporal stability and memory of local structural order fluctuations in quasi-two-dimensional dusty plasma liquids at the discrete limit.

In a two-dimensional (2D) liquid melted from a triangular lattice, the interparticle distance is still about the same as that of the solid due to the similar packing density. The increase of stochastic kicks with temperature induces the stick-slip avalanche particle hopping associated with clusters of a small number of particles out of the caging wells formed by the nearest-neighbor particles, and consequently the fluctuating structure of triangular lattice-type order domains with different lattice orientations separated by stringlike defect clusters (Fig. 1) [1,3,5–10]. It leads to interesting transport behaviors. For example, the non-Gaussian dynamics with anomalous diffusion under avalanche-type cooperative hopping, Stoke-Einstein relation, shear banding and shear thinning, etc., have been studied in the past few years [2,4–10]. Structuralwise, previous studies indicate that the power spectrum of the temporal fluctuations of the defect number in a fixed area and the histograms of defect and hopping cluster sizes all follow power-law distribution for the cold liquid. It reflects the correlation under the interplay of noise and mutual coupling [5–7]. Around each particle, the local structure can temporally fluctuate between an ordered state (with six nearest neighbors) and a disordered defect state (with nearest neighbors deviating from six) with persistence times t_o and t_d, respectively, through the creation, propagation, interaction, and annihilation of defects [1,6,7]. The structural memories and the capability of predicting the successive persistence times for local sites are still unexplored interesting issues.

The idea of persistence has been developed theoretically in recent years as a statistical measure for the stability and memory of extended nonequilibrium fluctuating systems, e.g., in the search for universal behavior in critical dynamics [11]. The persistence probability $P(t)$ is defined as the probability that a local variable remains above or below a certain reference level up to a persistence time t. Under stochastic drive, the memory in the non-Markov process is the key to change $P(t)$ from exponential to stretched exponential and power-law decay, which have been demonstrated in the recent studies of theoretical models such as diffusion, spin, Langevin equation, reaction-diffusion systems, interface, etc. [11–15], and a few experimental systems [15–18]. Nevertheless, the persistence behavior for the liquid at the discrete level has never been studied.

From a more general view, the caging barrier formed by the nearest neighbors sets up a threshold for the hopping excitation. The thermal induced avalanche-type stick-slip hopping of a cluster of a small number of particles makes the liquid at the discrete level belong to the general category of subexcitable coupled nonlinear extended systems, such as sand pile, earthquake system, chemical reaction diffusion systems, etc. They usually exhibit SOC- (self-organized criticality) type behaviors with heterogeneous avalanche activities after slowly accumulating local perturbation either from stochastic or persistent external drives beyond certain thresholds [5,6,19–21]. In addition to testing whether the generic scaling behaviors of the distributions of t_o and t_d for local structural order fluctuations of the microscopic liquid obey the universal trend, it is also interesting to use it as a paradigm to address the following generic correlation behaviors which has never been explored in any previous persistence studies [11–18]: (1) How are the persistence lengths of the same or the opposite states in different fluctuating cycles correlated (what kinds of length pairs are more or less likely

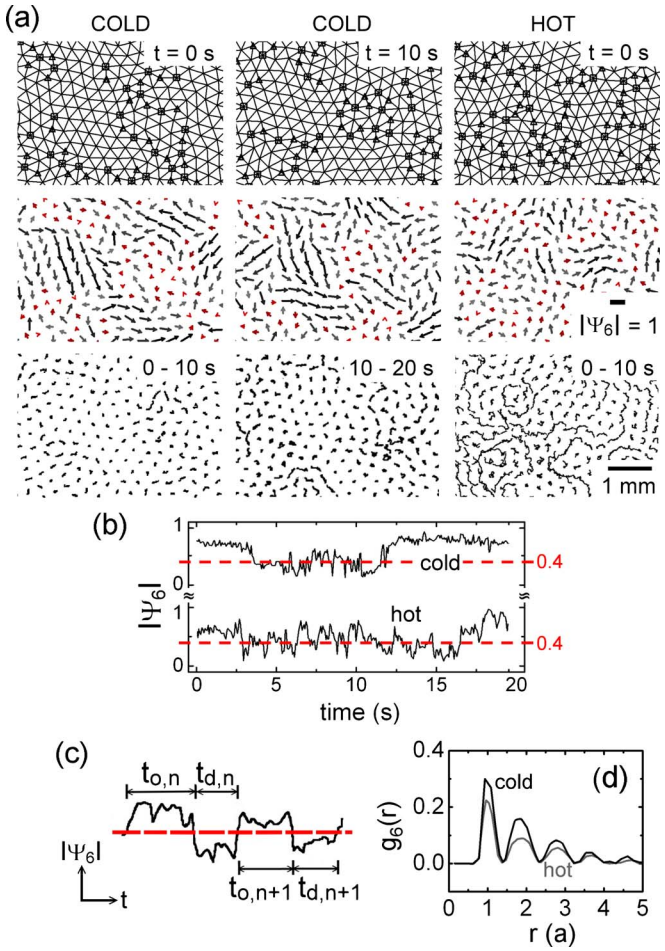

FIG. 1. (Color online) (a) The typical triangulated plots of the structures (top row), the corresponding Ψ_6 vectors (the second row) with the length and the orientation represent $|\Psi_6|$ and θ_6, respectively (the long black arrows represent the ordered sites), and the associated particle trajectories (third row), respectively. The left-hand two columns are from the cold run I at a different time, and the right-hand column is for the more disordered hot run II. (b) The temporal evolutions of $|\Psi_6|$ for typical sites in the cold and the hot runs. (c) The magnified plot of $|\Psi_6(t)|$ defining the persistence time in the successive cycles n and $n+1$. The dashed lines in (b) and (c) correspond to the reference at $|\Psi_6|=0.4$. (d) The radial pair correlation functions $g_6(r)=\langle\Psi_6(\mathbf{r_i})^*\Psi_6(\mathbf{r_j})\rangle$, averaged over pairs of Ψ_6 separated by distance r for the cold (black line) and the hot (gray line) runs, respectively.

to occur), through measuring their correlation probability? (2) How many fluctuation cycles can the correlation last? (3) How is the above memory carried?

In this work, using a 2D dusty plasma liquid, we experimentally study the above issues. Through tracking particle relative positions, the bond-orientational order (BOO) is used as a measure for local structural order [Fig. 1(a)] [21]. $\mathrm{BOO}=\Psi_6(\mathbf{r})=|\Psi_6|\exp(i\theta_6)=\frac{1}{N_r}\Sigma_i\exp(i6\theta_k)$, where θ_k is the angle of the bond from the particle at $\mathbf{r}$ to its nearest neighbor k, and N_r is the number of the nearest neighbors. $\theta_6/6$ is the effective bond orientation. $|\Psi_6|>0.4$ for an ordered site with six nearest neighbors and low strain, and $\leqslant 0.4$ for the disordered defect site with five or seven nearest neighbors and high strain. Using $|\Psi_6|=0.4$ as a reference threshold, we find that their persistence length t_o and t_d indeed both change from stretched exponential to power-law distribution as the liquid becomes colder, similar to other physical systems [11,14,16–18]. For the cold liquid, the persistence lengths of a sequence of alternating states, e.g., ordered-disordered-ordered (O-D-O) sequence or the D-O-D sequence, prefer alternating persistence length combinations, i.e., long-short-long (L-S-L) and short-long-short (S-L-S) combinations. The correlation memory lasts several O-D cycles and is shortened with increasing temperature. The correlation memory is carried in the surrounding network through mutual coupling. The interface region of the defect cluster and the order domain is more vulnerable to the fast switching.

II. EXPERIMENT

The experiment is conducted in a cylindrical symmetric discharged system as described elsewhere [5]. A weakly ionized discharge ($n_e\sim 10^9$ cm^{-3}) is generated in 250 mTorr Ar gas using a 14 MHz rf power system. Negatively charged polystyrene particles (each particle is charged to about 5000 electrons) at 7 μm diameter are suspended in the discharge in the hollow concentric cylindrical glass cell at 30 mm diameter placed on the floor of the vacuum system. The wake field of the downward ion flow causes the formation of vertical particle chains [22]. Each chain consists of eight particles. Particles in the same chain move together horizontally. The system can therefore be viewed as a quasi-2D system. The mean interchain distance a is 0.3 mm. The chain positions in the horizontal plane are illuminated by a thin horizontal laser sheet and tracked digitally at 15 Hz sampling rate through optical microscopy. The chain structure also suppresses vertical (out-of-viewing plane) particle motion. A slight change of particle number in each vertical chain causes little effect on the dynamical behavior. Fifty minutes of data are used for the statistical measurement. The degree of disorder of the liquid can be increased by increasing the rf power.

III. RESULTS AND DISCUSSIONS

We choose two typical runs, the cold run I and the hot run II with different radial correlation length and ordering obtained at 1.9 and 2.1 W rf power, respectively, as two typical examples for our study. The pair correlation lengths of the radial pair correlation functions $g_6(r)=\langle\Psi_6(\mathbf{r_i})^*\Psi_6(\mathbf{r_j})\rangle$, averaged over Ψ_6 obtained from pairs of particles i and j separated at distance r [Fig. 1(d)], shows the different degrees of ordering. Figure 1(a) shows their typical snapshots of the spatial configuration of defects and Ψ_6, and the particle trajectories. The triangles and squares represent the fivefold and sevenfold defects, respectively. The disordered (defect or the short Ψ_6 represented by red arrows) sites appear in the form of clusters. Namely, the thermal induced string- or vortex-type cooperative hopping induce structural fluctuation with defects and BOO fluctuations. Although the exact coupling constant is unknown due to the lack of the detailed measurements of temperature and charges, the size of the ordered

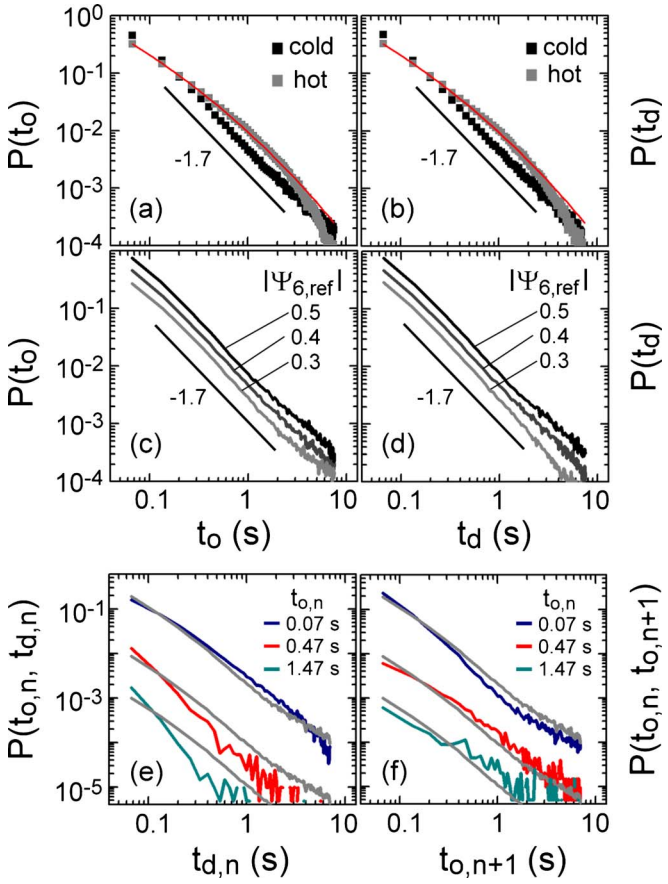

FIG. 2. (Color online) (a) and (b) The double logarithmic plots of the histograms of the persistence lengths t_o and t_d for the cold run showing the power-law decay and the hot run showing the stretched exponential decay, respectively. The (red) lines $[P(t_{o,d})=1.1\ \exp(-4.4t_{o,d}^{0.37})]$ are the best stretched exponential fitting for $P(t_o)$ and $P(t_d)$ of the hot run. $\Psi_{6,\mathrm{ref}}=0.4$ is used as the reference threshold for measuring the persistent time. (c) and (d) The double logarithmic plots of $P(t_o)$ and $P(t_d)$ for the cold run showing the negligible effect of the small variation of the reference threshold $|\Psi_{6,\mathrm{ref}}|$ from 0.3 to 0.5. (e) $P(t_{o,n},t_{d,n})$ (color lines) and the corresponding $P(t_{o,n})P(t_{d,n})$ (the three vertically shifted reference light gray lines) vs $t_{d,n}$ at several typical $t_{o,n}$ ($t_{o,n}$=0.07, 0.47, and 1.47 s from the top to the bottom curves, respectively) for the cold run. (f) $P(t_{o,n},t_{o,n+1})$ (color lines) and the corresponding $P(t_{o,n})P(t_{o,n+1})$ (the three vertically shifted reference light gray lines) vs $t_{o,n+1}$ at several typical $t_{o,n}$ ($t_{o,n}$=0.07, 0.47, and 1.47 s from the top to the bottom curves, respectively) for the cold run.

domain for cold run shows the cold run is close to the liquid with coupling constant equal to 129 around the solid-liquid transition from a 2D simulation [9]. The hot run II shows smaller size for the ordered domain surrounded by more defects under the more violent hopping (longer trajectories). It leads to the shorter correlation length in Fig. 1(d). Figures 1(b) and 1(c) show the typical temporal evolution of $|\Psi_6|$ and the definition of the temporal persistence length of a local site.

Figures 2(a) and 2(b) show that the persistence probabilities $P(t_o)$ and $P(t_d)$ both follow power-law decay with exponent $=-1.7$ for the cold run I, and nearly follow the stretched exponential decay except the faster drop at the tail part [see the (red) smooth best-fit curves with $P(t_{o,d})=1.1\ \exp(-4.4t_{o,d}^{0.37})$ in Figs. 2(a) and 2(b)], for the more disordered hot run II. This trend is similar to the behaviors observed in other physical systems [10,13,15,16]. Note that there are negligible effects on the scaling behaviors of $P(t_o)$ and $P(t_d)$ by changing the reference threshold for measuring t_o and t_d from 0.3 to 0.5 [Figs. 2(c) and 2(d)]. The three curves in each panel with different reference thresholds, $|\Psi_{6,\mathrm{ref}}|$, are intentionally shifted vertically in the plot in order to see the details. Before shifting, they fall nearly along the same curve.

The nonexponential decay in our above findings manifests that the temporal fluctuations of BOO are not completely disordered. There could be certain correlation between successive fluctuations. Due to the stochastic nature of the excitation source, we cannot exactly predict how long a disordered (ordered) state persists after an ordered (disordered) state with persistence time t_o (t_d). However, we can measure what kinds of persistence length combinations for sequential O-D pairs are more likely (unlikely) to occur from measuring the correlation probability $C(t_{o,n},t_{d,n})=P(t_{o,n},t_{d,n})-P(t_{o,n})P(t_{d,n})$, by subtracting the uncorrelated probability $P(t_{o,n})P(t_{d,n})$ from the joint probability $P(t_{o,n},t_{d,n})$ [see Fig. 1(c) for the definition of n and $n+1$]. Similarly, we also measure $C(t_{d,n},t_{o,n+1})$ for a D-O sequence. The three-dimensional (3D) and the corresponding contour plots of $C(t_{o,n},t_{d,n})$ and $C(t_{d,n},t_{o,n+1})$ in Figs. 3(a) and 3(b) show that, for O-D and D-O sequences, the L-S and S-L pairs are both preferred (i.e., with positive correlation) but the S-S and the L-L combinations are anticorrelated and unlikely to occur. The double logarithmic plots of $P(t_{o,n},t_{d,n})$ and $P(t_{o,n})P(t_{d,n})$ as a function of $t_{d,n}$ at several typical $t_{o,n}$ in Fig. 2(e) further show how they cross over with increasing $t_{d,n}$ and how the trend is inverted with increasing $t_{o,n}$. The transition from negative to positive correlation occurs between t_o (or t_d) $=0.1$ s and 0.17 s. The correlation follows the same trend but drops by sixfold for the hotter run II [Fig. 3(f)].

We further measure the correlation between the persistence lengths of the same type of states in different pairs of cycles n and $n+m$. For example, Fig. 2(f) shows the deviation of $P(t_{o,n},t_{o,n+1})$ from $P(t_{o,n})P(t_{o,n+1})$ as a function of $t_{o,n+1}$ at several typical $t_{o,n}$ for the cold run. The crossover behavior is opposite to that of $P(t_{o,n},t_{d,n})$ in Fig. 2(c), The plots of $C(t_{o,n},t_{o,n+1})$ [see Fig. 3(c)] and $C(t_{d,n},t_{d,n+1})$ [Fig. 3(e)] both indicate that S-S and L-L combinations are more likely to occur for two sequential ordered (or disordered) states. Similar correlation behavior is still maintained between the cycle n and cycle $n+m$ but with decreasing amplitude when m increases [Fig. 3(d)]. Figure 4 shows the dependence of $C(t_{o,n},t_{o,n+m})_{\max}$, the height of the highest peak in $C(t_{o,n},t_{o,n+m})$ plots, on m for the hot and the cold runs. With increasing m, $C(t_{o,n},t_{o,n+m})_{\max}$ decreases exponentially for the cold run and decreases faster than the exponential decay for the hot run. For example, it drops to 27% and 17% for the cold and the hot run, respectively, when m increases from 1 to 3. Note that $C(t_{o,n},t_{o,n+1})_{\max}$ decreases sixfold from the cold to the hot run.

The gradual decay of $C(t_{o,n},t_{o,n+m})_{\max}$ with increasing m reflects that the persistent memory can last several cycles.

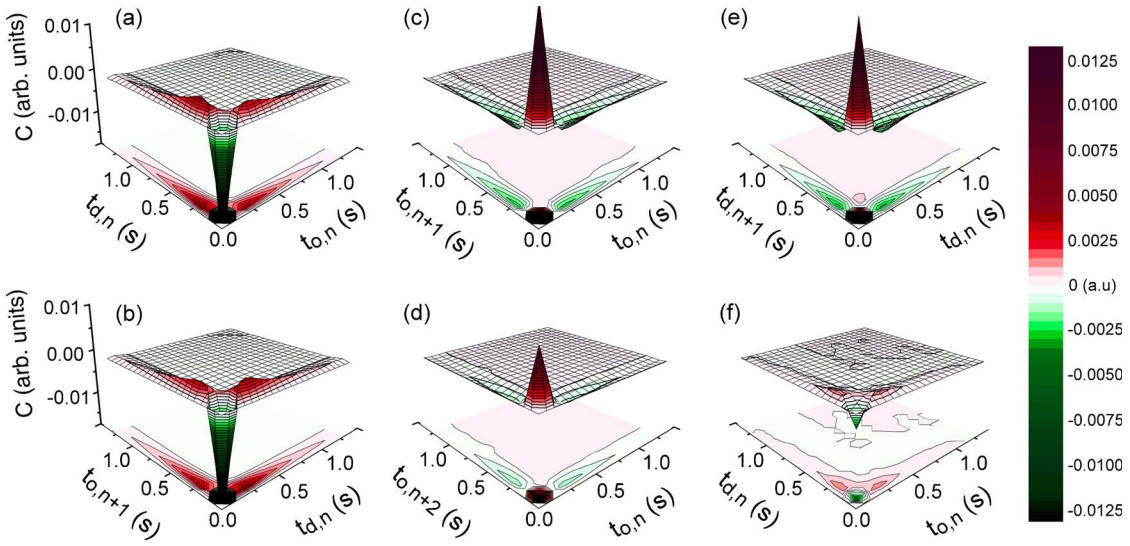

FIG. 3. (Color online) The 3D and the corresponding contour plots of the correlation probabilities C, for the pairs of $t_{o,n}$-$t_{d,n}$, $t_{d,n}$-$t_{o,n+1}$, $t_{o,n}$-$t_{o,n+1}$, $t_{o,n}$-$t_{o,n+2}$, and $t_{d,n}$-$t_{d,n+1}$ for the cold run I [(a) to (e)], and $t_{o,n}$-$t_{d,n}$ for the hot run II (f). Note that the correlation behavior for (f) for the hot run is similar to that of (a) for the cold run but with sixfold decrease of amplitude.

This gives a strong support for the non-Markov nature revealed by the power-law distribution of persistence time in the fluctuation processes. The correlation can be deteriorated and the distribution can be changed to the stretched exponential distribution and finally to exponential distribution (not shown) by increasing thermal agitation which washes out memory [11–15]. It is also manifested by the smaller $C(t_{o,n},t_{o,n+1})_{\max}$ and the faster decay of $C(t_{o,n},t_{o,n+m})_{\max}$ with increasing m for the hotter run.

The plots of mean square displacement (MSD) and temporal correlation of BOO, $g_6(\tau)=\langle\Psi_6(t+\tau)^*\Psi_6(t)\rangle$, in Fig. 5 shows the typical time scale for particle displacement and structural order evolution processes. At small time scale, the displacement is dominated by the thermal induced motion in the caging well formed by the surrounding nearest neighbors [5]. The diffusion is antipersistent with scaling exponent <1 in the double logarithmic plot of MSD versus τ. The small amplitude caged motion also induces very small change of Ψ_6. In the longer time regime, the accumulation of constructive perturbations from thermal agitations and the interaction from neighboring particles leads to avalanche-type coopera-

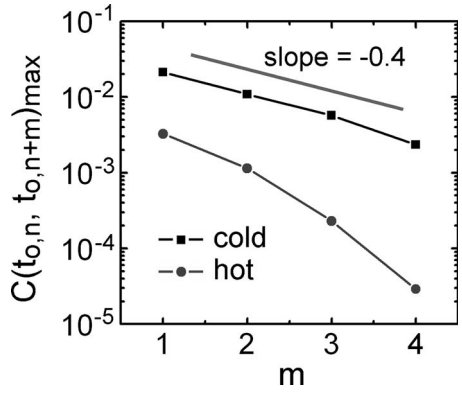

FIG. 4. The dependence of $C(t_{o,n},t_{o,n+m})_{\max}$, the height of the highest peak of the correlation amplitude for $C(t_{o,n},t_{o,n+m})$, on m, showing that the memory of persistence time lasts several fluctuating cycles. $C(t_{o,n},t_{o,n+m})_{\max}$ decreases exponentially for the cold run and shows a more drastic decay for the hot run with increasing m. For example, it drops to 27% and 17% for the cold and the hot run, respectively, when m increases from 1 to 3. Also note that $C(t_{o,n},t_{o,n+1})_{\max}$ for the hot run is 6 times smaller than that for the cold run.

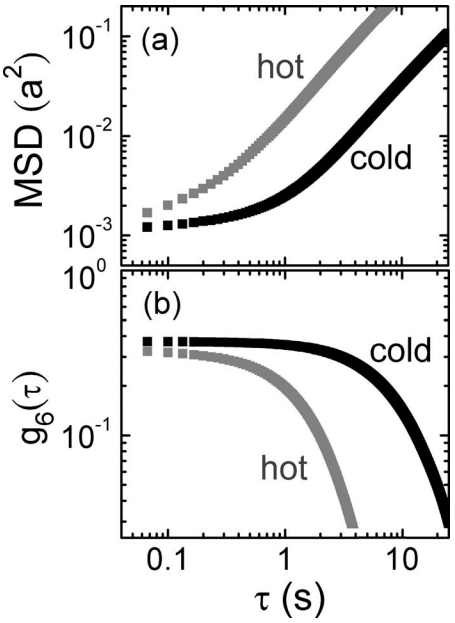

FIG. 5. The mean square displacement MSD(τ) and the temporal correlation of BOO, $g_6(\tau)=\langle\Psi_6(t+\tau)^*\Psi_6(t)\rangle$, where a is the mean interparticle distance. The upward bending of the MSD curves around 1 s and 0.3 s for the cold and the hot runs, respectively, evidences the transition from the caging dominated antipersistent diffusion to the hopping dominated persistent diffusion associated with structural rearrangement. The latter induces the drop of g_6 with the increasing τ, which reflects the gradual loss of structural memory.

tive hopping involving a cluster of a small number of particles [also see the trajectory plots in Fig. 1(a)]. It causes the persistent diffusion with scaling exponent of MSD greater than 1. The transition time τ_h, from caging dominated regime to hopping dominated regime occurs around 1 s and 0.3 s for the cold and the hot runs, respectively. The cooperative hopping also induces structural arrangement. Therefore $g_6(\tau)$ starts to deviate from the maximum value around τ_h and gradually drops with further increasing τ. It drops to 40% of the maximum value at 10 s and 1.7 s for the cold and the hot runs, respectively (i.e., at MSD $\sim 0.03a^2$). Namely, the structural memory is still partially retained within 10 s and 1.7 s for the cold and the hot run, respectively. This partial memory under the competition between mutual coupling which keeps the memory and stochastic noise drive which washes out memory leads to the observed persistence time distributions, and supports the faster structural memory loss for the hot run as depicted in Figs. 2–4.

The correlation measurement shows that the sequence of alternating states (e.g., D-O-D or the O-D-O sequences) prefers the L-S-L or S-L-S persistence length combination. Namely, if a site stays in an ordered or disordered state for a longer persistence time, it has a greater tendency to flip to the opposite state with shorter persistence time, then quickly return to the original state and stay there with another longer persistence time. It is less likely to directly switch to the opposite state and then stays there with long persistent time.

How is this correlation memory carried? Spatially, ordered domains are separated by disordered defect clusters to accommodate the different orientations of the ordered domains [Fig. 5(a)] [3–7]. The temporal evolutions of $|\Psi_6|$ of a few sites in the few typical regions are shown in Fig. 6(b). For the sites in the cores of the ordered domains and on the backbones of the disordered defect clusters (e.g., particle *A*, *B*, and *E*), the strong couplings from the neighboring sites at the same state induce very long ($\sim$10 s) persistent time. However, the sites around their boundaries (e.g., particle *C* and *D*) are affected by the competition from the two different groups of neighbors with opposite states. Their $|\Psi_6|$ [see those of particle *C* and *D* Fig. 5(b)] are closer to the reference level 0.4 than those in the core of their neighboring groups with opposite states. Under the stochastic thermal kicks, they are more likely to cross the reference level to the opposite states. Note that a hopping event which leads to the structural arrangement involving a cluster of particles usually persists for about 10 s [see the typical trajectory plots for the cold run in Fig. 1(a)]. The small persistent time scale for the middle state in a L-S-L sequence indicates that the flipping is not associated with avalanche-type hopping which also flip the states of neighboring particles together. The mother group in which they share the same original states still provides the stronger tie. Therefore, the site is quickly pulled back to the original states by its neighbors and remains there again for a long persistence time. It consequently induces the L-S-L sequence. The sites with black and gray dots in Fig. 6(a) correspond to those sites which have made the L-S-L/O-D-O and D-O-D events, respectively, in 4 s interval after the snapshot in Fig. 5(a), with the persistence time for the middle state shorter than 0.13 s. Namely, mutual coupling tends to make the neighboring sites alike. It is the major source for memory. It provides not only the correlation for the persistence lengths of the two sequential events but also the memory more than two O-D cycles for the sites around the interface of the ordered and disordered domain.

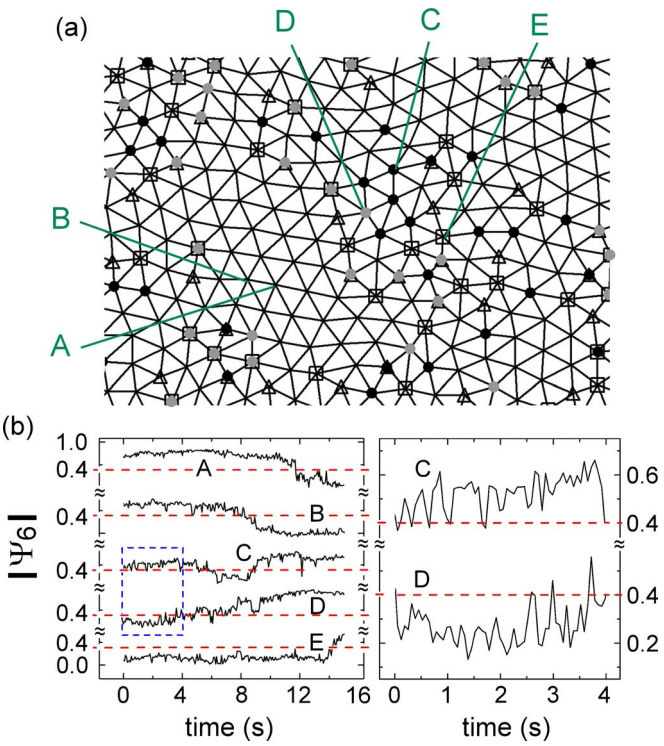

FIG. 6. (Color online) (a) The snapshot of the triangulated structure with sevenfold (squares) and fivefold (triangles) defects for the cold run. The sites with black and gray dots correspond to those sites which have made the L-S-L/O-D-O and L-S-L/D-O-D events, respectively, in the 4 s interval after the snapshot, with the persistence time for the middle state shorter than 0.13 s. They usually appear in the interface region between the temporally ordered domain and the defect clusters. (b) The temporal evolutions of $|\Psi_6|$ of a few typical sites in the above few typical regions after the snapshot in (a). The right-hand figure shows the more detailed temporal evolutions of $|\Psi_6|$ of particle *C* and *D* blown up from the dashed (blue) box region shown in the left-hand figure.

IV. CONCLUSION

In conclusion, we investigate the scaling behaviors and provide a new correlation measure to characterize the temporal persistence of microstructural order fluctuations in a dusty plasma liquid. For the cold liquid, power-law distributions of t_o and t_d are observed. The persistence lengths of the sequential fluctuations favor the L-S-L and S-L-S combination for both the O-D-O and the D-O-D sequences. The correlation can be carried over several O-D fluctuating cycles. The memory is stored in the neighboring network through mutual coupling. The fast switching to the opposite state and back is more likely to occur for the sites around the interface of the ordered domain and the backbone of the defect clusters through the competition from two sides with the opposite states. Namely, the portion of the neighboring particles at

the same state determines how vulnerable the noise-induced transition is to the opposite state. Increasing noise level deteriorates the memory, weakens the correlation, and induces the stretched exponential or even exponential distribution of the persistence length.

ACKNOWLEDGMENT

This work is supported by the National Science Council of the Republic of China under Contract No. NSC94-2112-M008-014.

[1] K. J. Strandberg, *Bond-Orientational Order in Condensed Matter Systems* (Springer, New York, 1992).
[2] M. C. Miguel, Nature (London) **410**, 667 (2001).
[3] F. L. Somer, G. S. Canright, T. Kaplan, K. Chen, and M. Mostoller, Phys. Rev. Lett. **79**, 3431 (1998).
[4] E. R. Weeks, J. C. Crocker, A. C. Levitt, A. Schofield, and D. A. Weitz, Science **287**, 627 (2000).
[5] Y. J. Lai and Lin I, Phys. Rev. Lett. **89**, 155002 (2002); W. T. Juan, M. H. Chen, and Lin I, Phys. Rev. E **64**, 016402 (2001).
[6] W. Y. Woon and Lin I, Phys. Rev. Lett. **92**, 065003 (2004); C. L. Chan, W. Y. Woon, and Lin I, *ibid.* **93**, 220602 (2004).
[7] C. Reichhardt and C. J. Olson Reichhardt, Phys. Rev. Lett. **90**, 095504 (2003).
[8] V. Nosenko and J. Goree, Phys. Rev. Lett. **93**, 155004 (2004).
[9] B. Liu, J. Goree, and O. S. Vaulina, Phys. Rev. Lett. **96**, 015005 (2006).
[10] S. Ratynskaia, K. Rypdal, C. Knapek, S. Khrapak, A. V. Milovanov, A. Ivlev, J. J. Rasmussen, and G. E. Morfill, Phys. Rev. Lett. **96**, 105010 (2006).
[11] For a review, see S. N. Majumdar, Curr. Sci. **77**, 370 (1999).
[12] A. J. Bray and S. J. O'Donoghue, Phys. Rev. E **62**, 3366 (2000).
[13] G. Manoj, Phys. Rev. E **67**, 026115 (2003).
[14] S. N. Majumdar and A. J. Bray, Phys. Rev. Lett. **91**, 030602 (2003); B. Derrida, V. Hakim, and V. Pasquier, *ibid.* **75**, 751 (1995).
[15] M. Constantin, S. Das Sarma, C. Dasgupta, O. Bondarchuk, D. B. Dougherty, and E. D. Williams, Phys. Rev. Lett. **91**, 086103 (2003).
[16] W. Y. Tam, R. Zeitak, K. Y. Szeto, and J. Stavans, Phys. Rev. Lett. **78**, 1588 (1997).
[17] G. P. Wong, R. W. Mair, R. L. Walsworth, and D. G. Cory, Phys. Rev. Lett. **86**, 4156 (2001).
[18] J. Merikoski, J. Maunuksela, M. Myllys, J. Timonen, and M. J. Alava, Phys. Rev. Lett. **90**, 024501 (2003).
[19] P. Bak, C. Tang, and K. Wiesenfeld, Phys. Rev. Lett. **59**, 381 (1987); H. J. Hensen, *Self-Organized Criticality* (Cambridge University Press, Cambridge, 1988).
[20] J. Wang, S. Kadar, P. Jung, and K. Showalter, Phys. Rev. Lett. **82**, 855 (1999).
[21] P. Bak, K. Christensen, L. Danon, and T. Scanlon, Phys. Rev. Lett. **88**, 178501 (2002).
[22] M. Nambu, S. V. Valdimirov, and P. K. Shukla, Phys. Lett. A **203**, 40 (1995).